Towards shape-oriented Bi-doped $CoCr_2O_4$ nanoparticles from theoretical and experimental perspective: Structural, Morphological, Optical, Electrical and Magnetic properties

K. Manjunatha[1,8], V. Jagadeesha Angadi[2*], M. C. Oliveira[3], S. R. de Lazaro[4], E. longo[5], R. A. P. Ribeiro[6*], S. O. Manjunatha,[7] N. H. Ayachith[9]

[1]*Department of Physics, School of Engineering, Presidency University, Bangalore-560064, India*

[2]*Department of Physics, P.C. Jabin Science College, Hubballi-580031, India*

[3]*LSQM – Laboratory of Chemical Synthesis of Materials – Department of Materials Engineering, Federal University of Rio Grande do Norte – UFRN, P.O. Box 1524, Natal RN, Brazil.*

[4]*Department of Chemistry, State University of Ponta Grossa, Av. General Carlos Cavalcanti, 4748, Zip code: 84030-900, Ponta Grossa, PR, Brazil*

[5]*CDMF-UFSCar, Universidade Federal de São Carlos, PO Box 676, 13565–905 São Carlos, SP, Brazil*

[6]*Department of Chemistry, Minas Gerais State University, Av. Paraná, 3001, Zip-Code: 35501-170, Divinópolis, MG, Brazil*

[7]*Department of Physics, FMPS, Ramaiah University of Applied Sciences, Bengaluru-560058, India*

[8]*Material Research Centre, School of Engineering, Presidency University, Bangalore-560064, India*

[9]*KLE Technological University, Hubballi-580031, India*

***Corresponding author: renan.ribeiro@uemg.br; jagadeeshbub@gmail.com**

Supporting Information

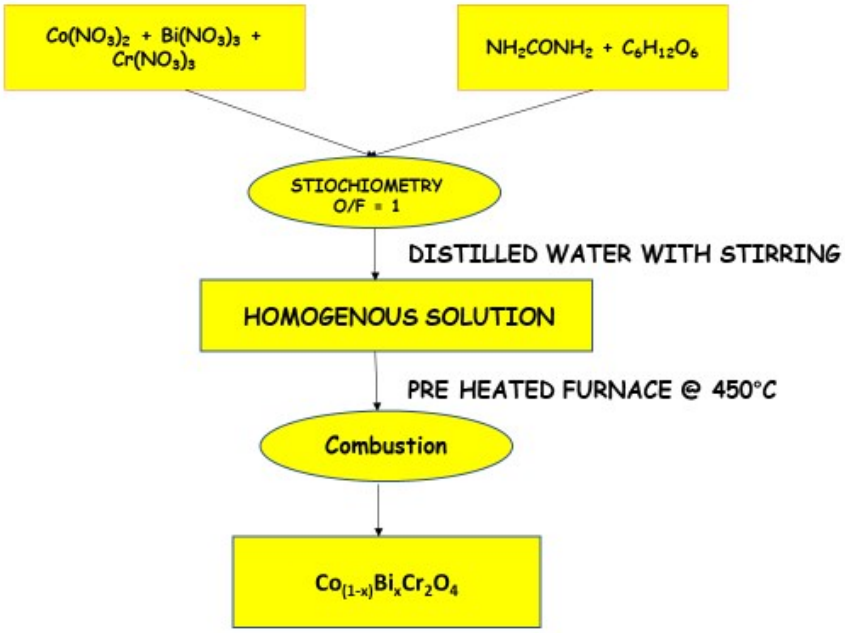

Figure S1: Solution combustion technique flow chart for $Co_{(1-x)}Bi_xCr_2O_4$ (where, x= 0.00, 0.05, 0.10) nanoparticles.

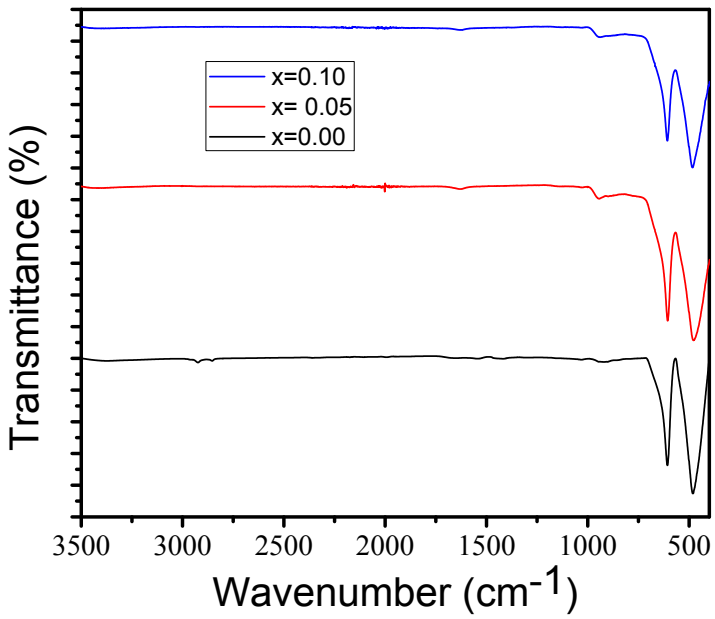

Figure S2: FTIR spectra of $Co_{(1-x)}Bi_xCr_2O_4$ (where, x= 0.00, 0.05, 0.10) nanoparticles

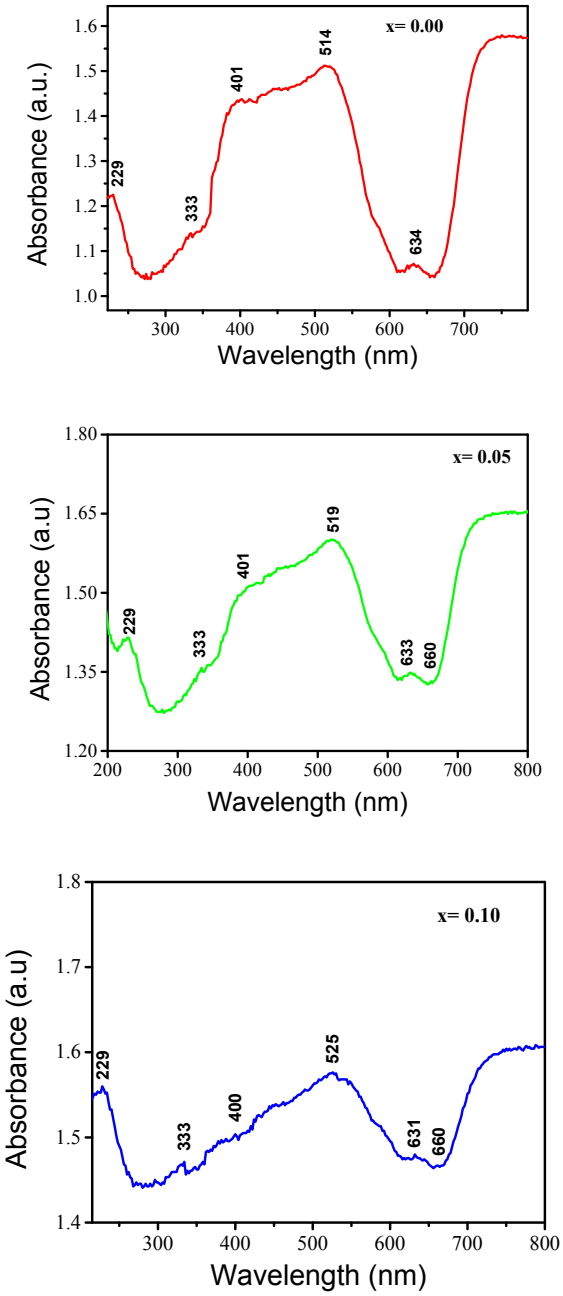

Figure S3: UV-Visible absorbance spectra of $Co_{(1-x)}Bi_xCr_2O_4$ (where, x= 0, 0.05, 0.10) nanoparticles

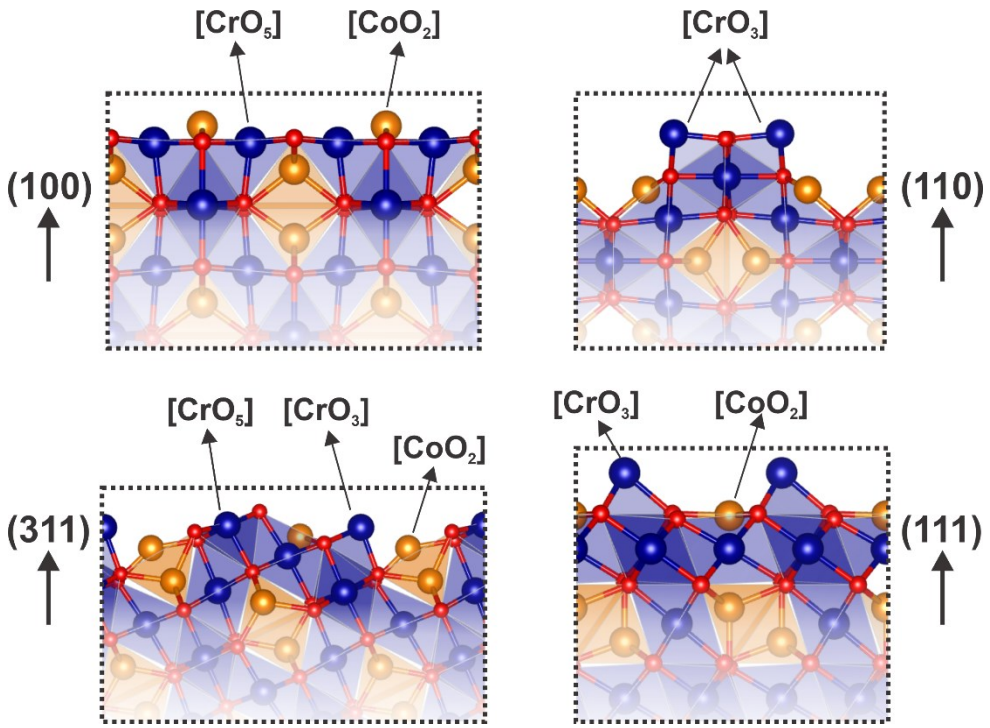

Figure S4. Schematic representation of chemical environment for $CoCr_2O_4$ (100), (110), (111), and (311) surfaces.

Table S1: Vibration bands, K_T and K_O values of $Co_{(1-x)}Bi_xCr_2O_4$ (where, x= 0.00, 0.05, 0.10) nanoparticles.

Bi^{3+} concentration	Vibration band (cm^{-1}) at the tetrahedral site	Vibration band (cm^{-1}) at octahedral site	K_T	K_O
x= 0	606.71	480.71	2.652×10^5	1.665×10^5
x= 0.05	604.93	478.78	2.636×10^5	1.651×10^5
x= 0.10	608.50	482.79	2.667×10^5	1.679×10^5

Table S2: EDS analysis of $Co_{(1-x)}Bi_xCr_2O_4$ (where, x= 0, 0.05, 0.10) nanoparticles

Identified elements	Theoretical stoichiometry	Experimental stoichiometry from EDS analysis
Cr	1	1
Co	1	1
Bi	0	0
Cr	1	1
Co	0.95	0.946
Bi	0.05	0.054
Cr	1	1
Co	0.90	0.8831
Bi	0.10	0.1168

Table S3. Calculated M-O bond distances in Å (M = Co, Sc, and Cr), bond length distortion indexes (Δ_d) in Å, and bond angle variances (BAV) in degree, for the pure and Bi-doped $CoCr_2O_4$ materials.

Models			M-O	Δ_d	BAV
$CoCr_2O_4$	$[CoO_4]$		1.995 (4x)	0.00	0.0
	$[CrO_6]$		1.994 (6x)	0.00	41.69
$Co_{(1-x)}Bi_xCr_2O_4$	$[CoO_4]$	Co(1)	1.994 (3x) 2.086 (1x)	0.01	10.30
		Co(2)	1.970 (1x) 2.010 (1x) 2.026 (2x)	0.01	5.28
		Co(3)	1.973 (2x) 2.008 (2x)	0.01	1.93
		Co(4)	1.992 (4x)	0.00	0.37
	$[BiO_4]$		2.180 (4x)	0.00	0.02
	$[CrO_6]$	Cr(1)	1.974 (1x) 1.986 (1x) 2.004 (2x) 2.019 (2x)	0.01	59.64
		Cr(2)	1.969 (1x) 1.989 (1x) 1.992 (1x) 1.997 (1x) 2.020 (2x)	0.01	57.70
		Cr(3)	1.950 (1x) 1.993 (2x) 2.012 (1x) 2.030 (2x)	0.01	49.06
		Cr(4)	1.929 (1x) 1.988 (1x) 1.992 (1x) 2.021 (1x) 2.039 (1x) 2.049 (1x)	0.02	75.81
		Cr(5)	1.901 (1x) 2.007 (2x) 2.012 (2x) 2.053 (1x)	0.02	48.36
		Cr(6)	1.965 (1x) 1.985 (2x) 2.009 (2x) 2.022 (1x)	0.01	33.42

Table S4. Calculated Surface Energy (J/m²) for (100), (110), (111) and (311) surfaces of $CoCr_2O_4$ as function of the Cr and Co chemical potential (eV).

(100)		***$\Delta\mu_{Co}$ (eV)***												
		-6	*-5.5*	*-5*	*-4.5*	*-4*	*-3.5*	*-3*	*-2.5*	*-2*	*-1.5*	*-1*	*-0.5*	*0*
$\Delta\mu_{Cr}$ (eV)	*-3*	2.06	1.95	1.83	1.72	1.60	1.49	1.38	1.26	1.15	1.03	0.92	0.80	0.69
	-2.5	2.06	1.95	1.83	1.72	1.60	1.49	1.38	1.26	1.15	1.03	0.92	0.80	0.69
	-2	2.06	1.95	1.83	1.72	1.60	1.49	1.38	1.26	1.15	1.03	0.92	0.80	0.69
	-1.5	2.06	1.95	1.83	1.72	1.60	1.49	1.38	1.26	1.15	1.03	0.92	0.80	0.69
	-1	2.06	1.95	1.83	1.72	1.60	1.49	1.38	1.26	1.15	1.03	0.92	0.80	0.69
	-0.5	2.06	1.95	1.83	1.72	1.60	1.49	1.38	1.26	1.15	1.03	0.92	0.80	0.69
	0	2.06	1.95	1.83	1.72	1.60	1.49	1.38	1.26	1.15	1.03	0.92	0.80	0.69
(110)		***$\Delta\mu_{Co}$ (eV)***												
		-6	*-5.5*	*-5*	*-4.5*	*-4*	*-3.5*	*-3*	*-2.5*	*-2*	*-1.5*	*-1*	*-0.5*	*0*
$\Delta\mu_{Cr}$ (eV)	*-3*	0.67	0.67	0.67	0.67	0.67	0.67	0.67	0.67	0.67	0.67	0.67	0.67	0.67
	-2.5	0.83	0.83	0.83	0.83	0.83	0.83	0.83	0.83	0.83	0.83	0.83	0.83	0.83
	-2	1.00	1.00	1.00	1.00	1.00	1.00	1.00	1.00	1.00	1.00	1.00	1.00	1.00
	-1.5	1.16	1.16	1.16	1.16	1.16	1.16	1.16	1.16	1.16	1.16	1.16	1.16	1.16
	-1	1.32	1.32	1.32	1.32	1.32	1.32	1.32	1.32	1.32	1.32	1.32	1.32	1.32
	-0.5	1.48	1.48	1.48	1.48	1.48	1.48	1.48	1.48	1.48	1.48	1.48	1.48	1.48
	0	1.64	1.64	1.64	1.64	1.64	1.64	1.64	1.64	1.64	1.64	1.64	1.64	1.64
(111)		***$\Delta\mu_{Co}$ (eV)***												
		-6	*-5.5*	*-5*	*-4.5*	*-4*	*-3.5*	*-3*	*-2.5*	*-2*	*-1.5*	*-1*	*-0.5*	*0*
$\Delta\mu_{Cr}$ (eV)	*-3*	0.77	0.77	0.77	0.77	0.77	0.77	0.77	0.77	0.77	0.77	0.77	0.77	0.77
	-2.5	0.90	0.90	0.90	0.90	0.90	0.90	0.90	0.90	0.90	0.90	0.90	0.90	0.90
	-2	1.03	1.03	1.03	1.03	1.03	1.03	1.03	1.03	1.03	1.03	1.03	1.03	1.03
	-1.5	1.16	1.16	1.16	1.16	1.16	1.16	1.16	1.16	1.16	1.16	1.16	1.16	1.16
	-1	1.30	1.30	1.30	1.30	1.30	1.30	1.30	1.30	1.30	1.30	1.30	1.30	1.30
	-0.5	1.43	1.43	1.43	1.43	1.43	1.43	1.43	1.43	1.43	1.43	1.43	1.43	1.43
	0	1.56	1.56	1.56	1.56	1.56	1.56	1.56	1.56	1.56	1.56	1.56	1.56	1.56
(311)		***$\Delta\mu_{Co}$ (eV)***												
		-6	*-5.5*	*-5*	*-4.5*	*-4*	*-3.5*	*-3*	*-2.5*	*-2*	*-1.5*	*-1*	*-0.5*	*0*
$\Delta\mu_{Cr}$ (eV)	*-3*	1.23	1.13	1.02	0.92	0.82	0.71	0.61	0.51	0.40	0.30	0.20	0.09	-0.01
	-2.5	1.37	1.26	1.16	1.06	0.95	0.85	0.75	0.64	0.54	0.44	0.33	0.23	0.13
	-2	1.51	1.40	1.30	1.20	1.09	0.99	0.89	0.78	0.68	0.58	0.47	0.37	0.27
	-1.5	1.64	1.54	1.44	1.33	1.23	1.13	1.02	0.92	0.82	0.71	0.61	0.51	0.40
	-1	1.78	1.68	1.57	1.47	1.37	1.26	1.16	1.06	0.95	0.85	0.75	0.64	0.54
	-0.5	1.92	1.82	1.71	1.61	1.51	1.40	1.30	1.20	1.09	0.99	0.89	0.78	0.68
	0	2.06	1.95	1.85	1.75	1.64	1.54	1.44	1.33	1.23	1.13	1.02	0.92	0.82